J Eng Math (2015) 92:31–44
DOI 10.1007/s10665-014-9763-9

On numerical modelling and the blow-up behavior of contact lines with a 180° contact angle

Dmitry E. Pelinovsky · Chengzhu Xu

Received: 23 May 2014 / Accepted: 29 October 2014 / Published online: 8 January 2015

Abstract We study numerically a reduced model proposed by Benilov and Vynnycky [J Fluid Mech 718:481–506, 2013], who examined the behavior of a contact line with a 180° contact angle between liquid and a moving plate, in the context of a two-dimensional Couette flow. The model is given by a linear fourth-order advection–diffusion equation with an unknown velocity, which is to be determined dynamically from an additional boundary condition at the contact line. The main claim of Benilov and Vynnycky is that for any physically relevant initial condition, there is a finite positive time at which the velocity of the contact line tends to negative infinity, whereas the profile of the fluid flow remains regular. Additionally, it is claimed that the velocity behaves as the logarithmic function of time near the blow-up time. Compared to the previous computations based on COMSOL built-in algorithms, we use MATLAB and develop a direct finite-difference method to study dynamics of the reduced model under different initial conditions. We confirm the first claim and also show that the blow-up behavior is better approximated by a power function, compared with the logarithmic function. This numerical result suggests a simple analytical explanation of the blow-up behavior of contact lines.

Keywords Advection–diffusion equation · Blow-up in a finite time · Numerical modelling

1 Introduction

Contact lines are defined by the triple-point intersection of the rigid boundary, fluid flow, and the vacuum state. Flows with the contact line at 180° contact angle were discussed in [1–3]. In the recent paper, Benilov and Vynnycky [4] analyzed the behavior of the contact line asymptotically using the thin-film equations. This latest contribution is a starting point for our work.

D. E. Pelinovsky (✉)
Department of Mathematics, McMaster University, Hamilton, ON L8S 4K1, Canada
e-mail: dmpeli@math.mcmaster.ca

D. E. Pelinovsky
Department of Applied Mathematics, Nizhny Novgorod State Technical University, Nizhny Novgorod, Russia

C. Xu
Department of Applied Mathematics, University of Waterloo, Waterloo, ON N2L 3G1, Canada

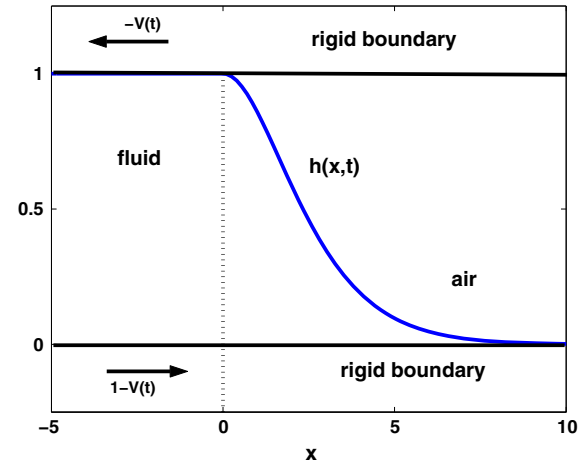

Fig. 1 A two-dimensional Couette flow with a free boundary, in the reference frame co-moving with the contact line

Let us consider a two-dimensional Couette flow shown in Fig. 1, where two horizontal rigid plates are separated by a distance normalized to unity, with the lower plate moving to the right relatively to the upper plate with a velocity normalized to unity. The space between the plates is filled with an incompressible fluid on the left, and vacuum (that is, gas with negligible density) on the right, separated by a free boundary. The x-axis is directed along the lower plate, and the contact line is located on the upper plate.

Physically relevant flows correspond to the configuration, where the fluid-filled region to the right of the contact line decays monotonically, and is carried away by the lower plate to some residual thickness h_∞ as $x \to \infty$. The velocity of the contact line is $V(t)$ and the reference frame in Fig. 1 moves to the left with the velocity $V(t)$ so that the contact line is placed dynamically at the point $x = 0$. Note that the velocity $V(t)$ is an unknown function of time t. The shape of the fluid–vacuum interface at time t is described by the graph of the function $y = h(x, t)$ for $x > 0$, where h is the thickness of the fluid-filled region.

Using asymptotic analysis and the lubrication approximation, Benilov and Vynnycky [4] derived the following nonlinear advection–diffusion equation for the free boundary $h(x, t)$ of the fluid flow:

$$\frac{\partial h}{\partial t} + \frac{\partial}{\partial x}\left[\frac{h^3}{3}\left(\alpha^3 \frac{\partial^3 h}{\partial x^3} + \frac{\partial h}{\partial x}\right) + (1 - V(t))h\right] = 0, \quad x > 0, \quad t > 0, \tag{1}$$

The boundary conditions $h|_{x=0} = 1$ and $h_x|_{x=0} = 0$ define the normalized thickness and the contact line location, whereas the flux conservation gives the boundary condition:

$$h_{xxx}\big|_{x=0} = -\frac{3}{2\alpha^3}.$$

Here and henceforth, we use the subscript to denote the partial derivative. Existence of weak solutions of the thin-film equation (1) for constant values of V and Neumann boundary conditions on a finite interval was recently shown by Chugunova et al. [5,6].

Using further asymptotic reductions with

$$h - 1 = \mathcal{O}\left(|V|^{-1}\right), \quad x = \mathcal{O}\left(|V|^{-1/3}\right), \quad t = \mathcal{O}\left(|V|^{-4/3}\right) \quad \text{as} \quad |V| \to \infty, \tag{2}$$

Benilov and Vynnycky [4] reduced the nonlinear equation (1) to the linear advection–diffusion equation:

$$\frac{\partial h}{\partial t} + \frac{\alpha^3}{3}\frac{\partial^4 h}{\partial x^4} = V(t)\frac{\partial h}{\partial x}, \quad x > 0, \quad t > 0, \tag{3}$$

subject to the boundary conditions

$$h\big|_{x=0} = 1, \quad h_x\big|_{x=0} = 0, \quad h_{xxx}\big|_{x=0} = -\frac{3}{2\alpha^3}, \quad t \geq 0. \tag{4}$$

Note that although Eq. (3) appears in the asymptotic reduction of Eq. (1) with the asymptotic scaling (2), the same variable h is used in both the equations. This is always possible, because Eq. (3) is invariant with respect to addition of a constant field. Also note that using a scaling transformation of the variables x and t, parameter α^3 can be scaled to be any positive number in the boundary-value problem (3)–(4). For convenience, we will set $\alpha^3 = 3$.

Physically relevant solutions correspond to monotonically decreasing solutions with $h \to h_\infty$ and $h_x, h_{xx} \to 0$ as $x \to \infty$, where $h_\infty < 1$. The asymptotic value h_∞ is not important, because any constant value of h_∞ is allowed thanks to the invariance of the linear advection–diffusion equation (3) with respect to addition of a constant field and a scaling transformation. Indeed, if $h(x, t)$ solves the boundary-value problem (3)–(4) such that $h \to 0$ as $x \to \infty$, then $\tilde{h}(\tilde{x}, \tilde{t})$ given by

$$\tilde{h}(\tilde{x}, \tilde{t}) = h_\infty + (1 - h_\infty)h(x, t), \quad \tilde{x} = (1 - h_\infty)^{1/3}x, \quad \tilde{t} = (1 - h_\infty)^{4/3}t, \tag{5}$$

for any $h_\infty < 1$, solves the same advection–diffusion equation (3) with the same boundary conditions (4) but with the variable velocity $\tilde{V}(\tilde{t}) = V(t)/(1 - h_\infty)$ and with the asymptotic behavior $h \to h_\infty$ as $x \to \infty$.

With three boundary conditions at $x = 0$ and the decay conditions for h as $x \to \infty$, the initial-value problem for Eq. (3) is over-determined and the third (over-determining) boundary condition at $x = 0$ is used to find the dependence of V on t. Local existence of solutions to the boundary-value problem (3)–(4) was proved by Pelinovsky et al. [7] using Laplace transform in x and the fractional power series expansion in powers of $t^{1/4}$.

We shall consider the time evolution of the boundary-value problem (3)–(4) starting with the initial data $h|_{t=0} = h_0(x)$ for a suitable function h_0. For physically relevant solutions, we assume that the profile $h_0(x)$ decays monotonically to a constant value as $x \to \infty$ and that 0 is a non-degenerate maximum of h_0 such that $h_0(0) = 1$, $h_0'(0) = 0$, and $h_0''(0) < 0$. The solution $h(x, t)$ may lose monotonicity in x during the dynamical evolution because the boundary value

$$\beta(t) := h_{xx}(0, t) \tag{6}$$

crosses zero from the negative side. In this case, we say that the flow becomes non-physical for further times and the model (3)–(4) breaks. Simultaneously, this may mean that the velocity $V(t)$ blows up to infinity, because for sufficiently strong solutions of the advection–diffusion equation (3), the velocity $V(t)$ satisfies the dynamical equation

$$h_{xxxxx}(0, t) = V(t)\beta(t), \tag{7}$$

which follows by differentiation of (3) in x and setting $x \to 0$.

Based on numerical computations of the thin-film equation (1), Benilov and Vynnycky [4] claim that for any physically relevant initial data h_0, there is a finite positive time t_0 such that $V(t)$ tends to negative infinity and $\beta(t)$ approaches zero as $t \nearrow t_0$, whereas the profile $h(x, t_0)$ remains a smooth and decreasing function for $x > 0$. Moreover, they claim that $V(t)$ behaves near the blow-up time as the logarithmic function of t:

$$V(t) \sim C_1 \log(t_0 - t) + C_2 \quad \text{as} \quad t \nearrow t_0, \tag{8}$$

where C_1, C_2 are positive constants. The same properties of the blow-up of contact lines were observed in [4] in numerical simulations of the reduced model (3)–(4). We point out that the numerical simulations in [4] are based on COMSOL built-in algorithms.

The goal of this paper is to simulate numerically the behavior of the velocity $V(t)$ near the blow-up time under different physically relevant initial data $h_0(x)$. Our technique is based on the reformulation of the boundary-value problem (3)–(4), which will be suitable for an application of the direct finite-difference method. We will approximate the behavior of the velocity $V(t)$ from the dynamical equation (7) rewritten in finite differences. The numerical computations reported in this paper were performed using the MATLAB.

As the main outcome of our work, we confirm numerically that all physically relevant initial data including those with positive initial velocity will result in the blow-up of $V(t)$ to negative infinity in a finite time. At the same time, we show that the power function

$$|V(t)| \sim \frac{c}{(t_0 - t)^p} \quad \text{as} \quad t \nearrow t_0 \tag{9}$$

with $c > 0$ and $p \approx 0.5$ fits our numerical data better than the logarithmic function (8) near the blow-up time t_0. We also explain analytically why the behavior $|V(t)| = \mathcal{O}((t_0 - t)^{-1/2})$ as $t \nearrow t_0$ is highly anticipated for solutions of the boundary-value problem (3)–(4). We believe that the incorrect logarithmic law (8) is an artifact of the COMSOL built-in algorithms used in [4].

We shall mention two recent relevant works on the same problem. Firstly, existence of self-similar solutions of the linear advection–diffusion equation (3) was proved by Pelinovsky and Giniyatullin [8]. The self-similar solutions are given by

$$V(t) = \frac{t_0 V_0}{(t_0 - t)^{3/4}}, \quad h(x,t) = f(\xi), \quad \xi = \frac{x}{(t_0 - t)^{1/4}}, \tag{10}$$

with $t_0 > 0$ and $V_0 > 0$, where $f(\xi)$ is a suitable function. Although the self-similar solutions (10) satisfy the decay condition at infinity, and the first two boundary conditions (4), the third boundary condition is not satisfied and is replaced with $h_{xxx}|_{x=0} = \gamma_0 V(t)$ for a fixed $\gamma_0 < 0$. Consequently, the self-similar solution (10) predicts singularities in a finite time with positive $V(t)$ and positive $\beta(t)$. Although the scaling of the self-similar solution (10) is compatible with the scaling transformation (2) used in the derivation of the linear advection–diffusion equation (3), it does not satisfy the physical requirements of the Couette flow shown in Fig. 1.

Secondly, Chugunova et al. [9] constructed steady-state solutions of the boundary-value problem (3)–(4) and showed numerically that these steady states can serve as attractors of the bounded dynamical evolution of the model. Both the steady states and the initial conditions that lead to bounded dynamics of the model are not physically acceptable as h_0 has to be monotonically increasing with $h \to h_\infty > 1$ as $x \to \infty$. Note that both V and β are positive for the steady states of the boundary-value problem (3)–(4).

Both recent works of [8] and [9] used a priori energy estimates and found some sufficient conditions, under which the smooth physically relevant solutions of the boundary-value problem (3)–(4) blow up in a finite time. In particular, if $V(t) > -1$, or $\beta(t) < 0$, or $V(t)\beta(t)^2 < 0$, the smooth solution $h(x,t)$ blows up in a finite time. However, these sufficient conditions do not eliminate the existence of smooth physically relevant solutions, for which $V(t)$ oscillates and $\beta(t)$ decays to zero as $t \to \infty$.

To simulate the boundary-value problem (3)–(4), a different numerical method is proposed in [9]. Similar to our work, this method is based on finite differences using MATLAB. Because the fourth-order derivative term is approximated implicitly and the first-order derivative term is approximated explicitly, the system of finite-difference equations is closed in [9] without any additional equation on the velocity $V(t)$.

Compared to the finite-difference method used in [9], we determine the velocity $V(t)$ from the finite-difference approximation of the dynamical equation (7). This provides additional accuracy in the detection of $V(t)$ near the blow-up time. We also derive constraints on the smooth solutions of the boundary-value problem (3)–(4) and use them to measure the error of numerical approximations in our simulations. In addition, we control the accuracy of the numerical solution using the method of dynamical rescaling of the time variable, which was earlier used in [4].

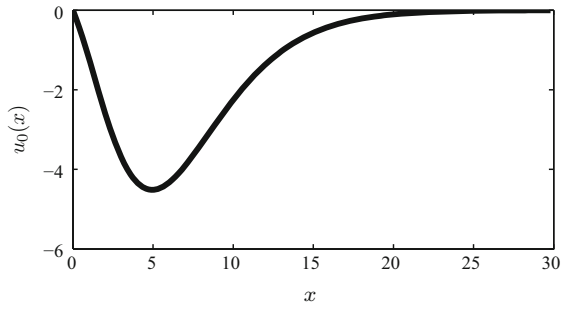

Fig. 2 The initial function (14) with $a = 0.5$ and $b = 0$

The remainder of our paper is organized as follows: Section 2 outlines the numerical method for approximations of the boundary-value problem (3)–(4). Section 3 presents the numerical simulations of the boundary-value problem truncated on the finite interval $[0, L]$ for sufficiently large L. Section 4 inspects different blow-up rates of the singular behavior of the velocity $V(t)$ near the blow-up time. Section 5 summarizes our findings.

2 Numerical method

In what follows, we set $u := h_x$ and reformulate the boundary-value problem (3)–(4) in the equivalent form. Differentiating Eq. (3) with $\alpha^3 = 3$ with respect to x, we obtain

$$\frac{\partial u}{\partial t} + \frac{\partial^4 u}{\partial x^4} = V(t)\frac{\partial u}{\partial x}, \quad x > 0, \quad t > 0. \tag{11}$$

We also rewrite boundary conditions in (4) with $\alpha^3 = 3$ as follows:

$$u\big|_{x=0} = 0, \quad u_{xx}\big|_{x=0} = -\frac{1}{2}, \quad u_{xxx}\big|_{x=0} = 0, \quad t \geq 0. \tag{12}$$

Here the third boundary condition $u_{xxx}|_{x=0} = h_{xxxx}|_{x=0} = 0$ follows from applying the boundary conditions $h|_{x=0} = 1$ and $h_x|_{x=0} = 0$ to the fourth-order equation (3) as $x \to 0$. After the reformulation, the dynamical equation (7) can be recovered by taking the limit $x \to 0$ in (11):

$$u_{xxxx}(0, t) = V(t)u_x(0, t), \quad t \geq 0, \tag{13}$$

provided that the solution u remains smooth at the boundary $x = 0$.

A suitable two-parameter initial condition $u|_{t=0} = u_0(x)$ for the boundary-value problem (11)–(12) can be chosen in the form

$$u_0(x) = -\frac{1}{4}x\left(4 + (4a + 1)x + a(2a + 1)x^2 + bx^3\right)\mathrm{e}^{-ax}, \tag{14}$$

where parameters $a > 0$ and $b \geq 0$ are arbitrary. For simplicity, the constraint

$$\beta(t) = h_{xx}\big|_{x=0} = u_x\big|_{x=0} < 0$$

at the initial time $t = 0$ is standardized to $\beta(0) = -1$. Note that $u_0(x)$ and its derivatives decay to zero exponentially fast as $x \to \infty$, which still imply that $h_0(x) = 1 + \int_0^x u_0(x')\mathrm{d}x'$ decays to some constant value h_∞ as $x \to \infty$. Because $u_0(x) < 0$ for all $x > 0$, h_0 is a monotonically decreasing function and $h_\infty < 1$. Figure 2 shows a particular example of the initial function (14) for $a = 0.5$ and $b = 0$.

We approximate solutions of the boundary-value problem (11)–(12) with the second-order central-difference method. Consider a set of $N+2$ equally spaced ordered grid points $\{x_n\}_{n=0}^{N+1}$ on the interval $[0, L]$, for sufficiently large L so that $u|_{x=L}$ and $u_{xx}|_{x=L}$ are approximately zero. For any fixed $t > 0$, $u_n(t)$ denotes the numerical approximation of $u(x,t)$ at $x = x_n$, and Δx denotes the constant spacing between adjacent grid points. In our numerical simulations, we use $L = 30$ and $N = 149$ for computational efficiency at the desired accuracy.

By applying the second-order central-difference formulas to partial derivatives in the fourth-order equation (11) at each $x = x_n$, we obtain the differential equations:

$$\frac{\mathrm{d}u_n}{\mathrm{d}t} = V(t)\frac{u_{n+1} - u_{n-1}}{2\Delta x} - \frac{u_{n+2} - 4u_{n+1} + 6u_n - 4u_{n-1} + u_{n-2}}{\Delta x^4}, \tag{15}$$

which are accurate up to the $\mathcal{O}(\Delta x^2)$ truncation error. Since $u_0 = u(0,t) = 0$ and $u_{N+1} = u(L,t) = 0$ for all $t \geq 0$, the above formula needs only to be applied to N interior points $\{x_n\}_{n=1}^{N}$ with the necessity to approximate u_{-1} for an equation at the grid point x_1 and u_{N+2} for an equation at the grid point x_N. The value of u_{-1} can be found from the boundary condition:

$$u_{xx}\big|_{x=0} = -\frac{1}{2} \quad \Rightarrow \quad \frac{u_{-1} - 2u_0 + u_1}{\Delta x^2} = -\frac{1}{2} \quad \Rightarrow \quad u_{-1} = -u_1 - \frac{1}{2}\Delta x^2,$$

and u_{N+2} can be found from the decay condition:

$$u_{xx}\big|_{x=L} = 0 \quad \Rightarrow \quad \frac{u_N - 2u_{N+1} + u_{N+2}}{\Delta x^2} = 0 \quad \Rightarrow \quad u_{N+2} = -u_N,$$

which are again accurate up to the $\mathcal{O}(\Delta x^2)$ truncation error. It remains to define $V(t)$ and to use the third boundary condition $u_{xxx}|_{x=0} = 0$.

The velocity $V(t)$ can be expressed by applying the central-difference approximation to the dynamical equation (13):

$$V(t) = \frac{u_{xxxx}\big|_{x=0}}{u_x\big|_{x=0}} \quad \Rightarrow \quad V(t) = \frac{2(u_2 - 4u_1 + 6u_0 - 4u_{-1} + u_{-2})}{(u_1 - u_{-1})\Delta x^3}, \tag{16}$$

where u_{-2} can be found from the third boundary condition in (12):

$$u_{xxx}\big|_{x=0} = 0 \quad \Rightarrow \quad \frac{u_2 - 2u_1 + 2u_{-1} - u_{-2}}{\Delta x^3} = 0 \quad \Rightarrow \quad u_{-2} = u_2 - 4u_1 - \Delta x^2.$$

Writing the system of differential equations (15) in the matrix form

$$\frac{\mathrm{d}\boldsymbol{u}}{\mathrm{d}t} = \boldsymbol{A}\boldsymbol{u} + \boldsymbol{b},$$

we use Heun's method to evaluate solutions of the system of differential equations. Let $\boldsymbol{u}_k$ denote the numerical approximation of $\boldsymbol{u}(t)$ at $t = t_k$ and let Δt denote the time step size (not necessarily constant). By the explicit Heun's method, we obtain the iterative rule

$$\boldsymbol{u}_{k+1} = \boldsymbol{u}_k + \frac{\Delta t}{2}\left[(\boldsymbol{A}_k\boldsymbol{u}_k + \boldsymbol{b}) + (\boldsymbol{A}_{k+1}\boldsymbol{u}_{k+1} + \boldsymbol{b})\right], \tag{17}$$

where the initial vector $\boldsymbol{u}_0$ is obtained from the initial condition (14). Note that the coefficient matrix $\boldsymbol{A}$ depends on t since it is defined by the variable velocity $V(t)$. Nevertheless, $\mathbf{b}$ is constant in t. The global error of Heun's method is $\mathcal{O}(\Delta t^2)$, so the global truncation error for the numerical approximation is $\mathcal{O}(\Delta x^2 + \Delta t^2)$.

In order to achieve better stability in the time stepping, the implicit Heun's method is employed. This method is stable for all $\Delta t > 0$, and hence the time step sizes are not as limited as in explicit methods. Thus, it provides potential for better computational efficiency. In the implicit Heun's method, the system of linear equations to be solved is

$$\left(\boldsymbol{I} - \frac{\Delta t}{2}\boldsymbol{A}_{k+1}\right)\boldsymbol{u}_{k+1} = \left(\boldsymbol{I} + \frac{\Delta t}{2}\boldsymbol{A}_k\right)\boldsymbol{u}_k + \Delta t\boldsymbol{b}, \tag{18}$$

where $\boldsymbol{I}$ is the identity matrix. However, because the coefficient matrix $\boldsymbol{A}_{k+1}$ on the left-hand side contains an unknown value of $V(t_{k+1})$, a prediction-correction method is necessary for solving this system of equations as follows: First, $\boldsymbol{A}_{k+1}$ is approximated using $\boldsymbol{A}_k$ to predict the value of $\boldsymbol{u}^*_{k+1}$ using Eq. (18), which is then used to predict the value of $V(t^*_{k+1})$ using Eq. (16). Second, $\boldsymbol{A}_{k+1}$ is updated from the prediction $V(t^*_{k+1})$ to obtain the corrected values of $\boldsymbol{u}_{k+1}$ and $V(t_{k+1})$ from Eqs. (18) and (16), respectively. Since the implicit method is used in both prediction and correction steps, the unconditional stability is preserved.

3 Blow-up of the velocity V of contact lines

We use the finite-difference method to compute approximation of the boundary-value problem (11)–(12), after truncation on the finite interval $[0, L]$ with $L = 30$. Since the time evolution features blow-up in a finite time, an adaptive method is used to adjust the time step Δt after each iteration to maintain the local truncation error of the numerical method at a certain tolerance level.

Figure 3 shows the numerical approximation of the boundary-value problem (11)–(12) for the initial function (14) with $a = 0.5$ and $b = 0$ (the one shown in Fig. 2). The initial velocity is determined from this initial condition by Eq. (13) as $V(0) = -1.25$. Panel (a) of the figure shows the profile of $u(x, t)$ versus x at different values of t until the terminal time of our computations. Panel (b) of the figure shows the change of the velocity $V(t)$ in time t computed dynamically from Eq. (16). Panels (c) and (d) show the boundary values $\beta(t) = u_x|_{x=0}$ and $u_{xxxx}|_{x=0}$ versus t.

It is clear from Fig. 3a and b that the velocity V diverges toward $-\infty$ at $t \approx 1.9$, whereas the solution $u(x, t)$ remains regular near the blow-up time. Recall that the velocity $V(t)$ is determined from Eq. (13) by the quotient of $u_{xxxx}(0, t)$ and $\beta(t) = u_x(0, t)$, where $\beta(t)$ must be strictly negative for all $t > 0$ for physically acceptable solutions. It is also seen from Fig. 3c and d that the value of β is about to cross zero from the negative side at the blow-up time, whereas $u_{xxxx}(0, t)$ also approaches zero but at a much slower rate than $\beta(t)$. This also indicates that $V(t)$ approaches negative infinity at the blow-up time.

To measure the error of numerical computations, we shall derive dynamical constraints on the time evolution of a smooth solution of the boundary-value problem (11)–(12). Differentiating Eq. (11) with respect to x once and twice and taking the limit $x \to 0$, we obtain

$$\frac{\mathrm{d}\beta}{\mathrm{d}t} + \left.\frac{\partial^5 u}{\partial x^5}\right|_{x=0} = -\frac{1}{2}V(t) \tag{19}$$

and

$$\left.\frac{\partial^6 u}{\partial x^6}\right|_{x=0} = 0. \tag{20}$$

Using Eq. (20), we determine u_{-3} at $x = x_{-3}$ from the central-difference approximation:

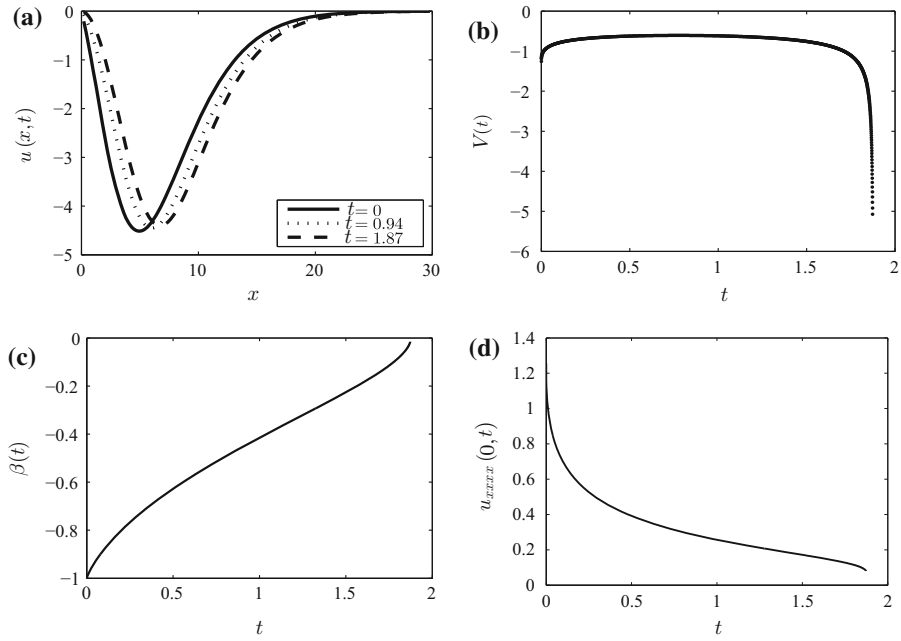

Fig. 3 Numerical solution of the boundary-value problem (11)–(12), where u_0 is given by (14) with $a = 0.5$ and $b = 0$. **a** The profile of u versus x at different time t. **b** Velocity of the contact line V versus t. **c** The boundary value $\beta = u_x|_{x=0}$ versus t. **d** The boundary value $u_{xxxx}|_{x=0}$ versus t

$$\frac{u_3 - 6u_2 + 15u_1 - 20u_0 + 15u_{-1} - 6u_{-2} + u_{-3}}{\Delta x^6} = 0 \quad \Rightarrow \quad u_{-3} = -u_3 + 12u_2 - 24u_1 + \frac{3}{2}\Delta x^2.$$

Then, the derivative of $\beta(t)$ is approximated from Eqs. (16) and (19):

$$\beta'(t) = -\frac{u_3 - 4u_2 + 5u_1 - 5u_{-1} + 4u_{-2} - u_{-3}}{2\Delta x^5} - \frac{u_2 - 4u_1 + 6u_0 - 4u_{-1} + u_{-2}}{(u_1 - u_{-1})\Delta x^3}. \tag{21}$$

Comparing the value of $\beta'(t)$ determined from Eq. (21) with the central-difference approximation for the numerical derivative

$$\beta'(t_l) = \frac{\beta(t_{k+1}) - \beta(t_{k-1})}{t_{k+1} - t_{k-1}}, \tag{22}$$

we can estimate the numerical error of the solution at the boundary $x = 0$.

Figure 4a compares the value of $\beta'(t)$ between Eqs. (21) and (22). The error remains small; therefore, the assumption that the solution is smooth at the boundary $x = 0$ is valid up to numerical accuracy. Figure 4b shows the time step size Δt adjusted to preserve the same tolerance level of 10^{-5} in the standard error estimation procedure for Heun's methods. We set $\Delta t = 0.006$ if the error estimation procedure yields larger values of Δt. This truncation is needed because the error drops significantly near $t \approx 0.8$, and the error estimation procedure would otherwise produce large values of Δt.

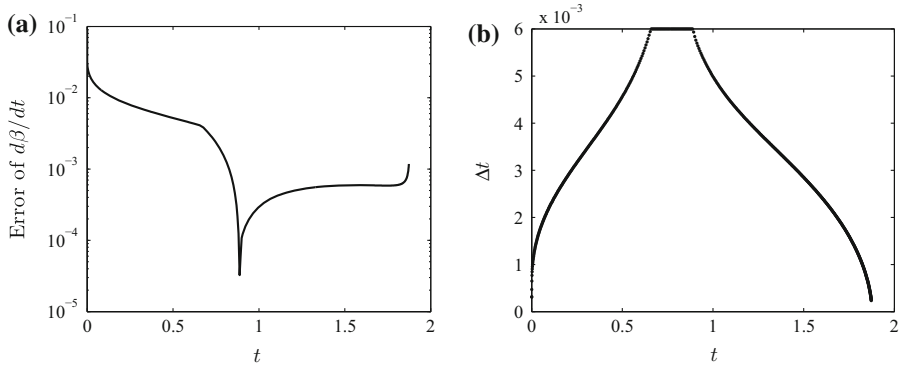

Fig. 4 **a** Error of $\beta'(t)$ versus t. **b** Time step size Δt versus t

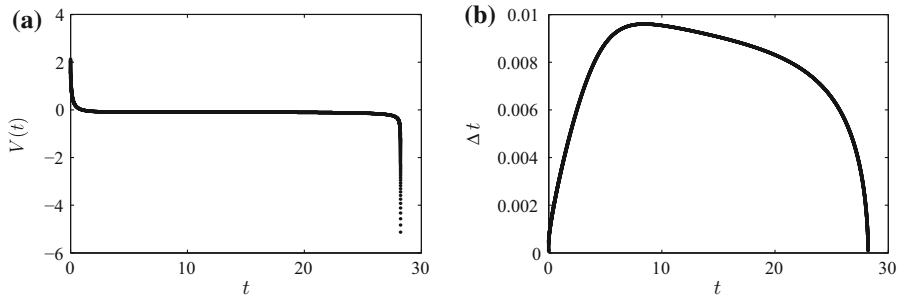

Fig. 5 Numerical solution of the boundary-value problem (11)–(12), where u_0 is given by (14) with $a = 0.5$ and $b = 0.6$. **a** Velocity of the contact line V versus t. **b** Time step size Δt versus t

We have performed computations with other initial conditions from the two-parameter family of functions in (14). Figure 5a shows the dynamical evolution of the velocity V starting with a positive velocity $V(0) = 2.35$, which is determined from the initial function (14) with $a = 0.5$ and $b = 0.6$. Although the terminal time is much larger compared with the case of the negative initial velocity as shown in Fig. 3, a blow-up is still detected from this initial condition. The solution $u(x, t)$ looks similar to the solution shown in Fig. 3a and hence is not shown.

Figure 5b shows the adjusted time step size. We note that the time step size is small at the initial time because a smooth solution of the boundary-value problem (11)–(12) appears from the initial condition u_0, which does not satisfy the infinitely many constraints such as (13), (19), and (20). It is also small near the terminal time because of the blow-up of the smooth solution. But Δt is not too small at intermediate values of t when the solution is at a slowly varying phase. During this slowly varying phase, $V(t)$ is nearly constant but $\beta(t)$ changes nearly linearly in time (similar to Fig. 3c and hence is not shown).

Figure 6 illustrates the dynamical evolution of the velocities $V(t)$ under different initial conditions given by the two-parameter function (14). From these plots, together with the previous examples, it is clear that the blow-up time depends on the initial velocity $V(0)$ and a large positive initial velocity leads to a much longer slowly varying phase before the solution blows up. Nevertheless, the blow-up in a finite time is inevitable for all physically acceptable initial conditions.

4 Rate of blow-up

In order to determine numerically the blow-up time t_0 and the rate of blow-up of the velocity V, we will fit the numerical data near the blow-up time with either the logarithmic function (8) or the power function (9).

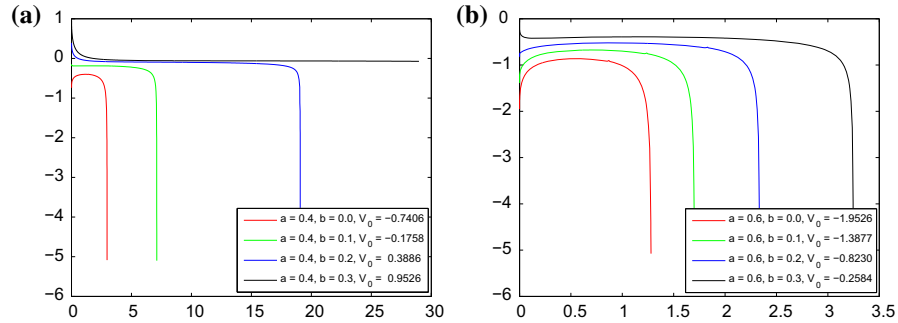

Fig. 6 Behavior of the velocity V versus t for different initial conditions given by the two-parameter function (14). **a** $a = 0.4$, **b** $a = 0.6$

For the logarithmic function (8), we first differentiate both sides of the expression with respect to t and take the inverse:

$$\frac{\mathrm{d}V}{\mathrm{d}t} = -\frac{C_1}{t_0 - t} \quad \Rightarrow \quad \left(\frac{\mathrm{d}V}{\mathrm{d}t}\right)^{-1} = \frac{t}{C_1} - \frac{t_0}{C_1}. \tag{23}$$

Then the constants C_1 and t_0 can be determined from a linear regression applied to the data points for $(\mathrm{d}V/\mathrm{d}t)^{-1}$. We will skip the numerical procedure for determining the values of C_2 since it does not affect the blow-up behavior of V.

For the power function (9), we can take the logarithm of both sides of the expression

$$\log(-V(t)) = \log c - p \log(t_0 - t)$$

and then differentiate the above expression:

$$\frac{1}{V(t)}\frac{\mathrm{d}V}{\mathrm{d}t} = \frac{p}{t_0 - t} \quad \Rightarrow \quad V(t)\left(\frac{\mathrm{d}V}{\mathrm{d}t}\right)^{-1} = \frac{t_0}{p} - \frac{t}{p}. \tag{24}$$

The constants p and t_0 can now be determined from a linear regression applied to the data points for $V(\mathrm{d}V/\mathrm{d}t)^{-1}$.

In practice, we found that the blow-up rate p in the power law or the coefficient C_1 in the logarithmic law varies with different time windows (i.e., the range of t which is used to fit the data). Table 1 gives a comparison of numerical data under different time windows and different tolerance levels, using the initial condition (14) with $a = 0.5$ and $b = 0$. Here *starting time* means the time t at which we start to fit the data, and *error* is the mean squared error (MSE) defined by

$$\mathrm{MSE} := \frac{1}{n-3}\sum (V_{\mathrm{obs}} - V_{\mathrm{fit}})^2,$$

where n is the total number of data points used in the regression and $n - 3$ is the degree of freedom.

Table 1 shows that the errors from the logarithmic law (8) are much larger than the errors from the power law (9) in all cases. Also, the error of the power law reduces as the time window moves closer to the blow-up time, whereas the error of the logarithmic law increases. Moreover, the blow-up times t_0 determined from the logarithmic law are smaller than the terminal time of our computations. Hence, the logarithmic law deviates from the numerical data near the blow-up time. As we can see in Fig. 7, the power function (9) fits our numerical data much better than the logarithmic function (8).

Table 1 Data for two sets of numerical computations

Method	Starting time	Blow-up time t_0	Blow-up rate p or C_1	Error
(a) Tolerance level: 10^{-4}, number of iterations: 330, terminal time: 1.8729				
Power law	1.8176	1.8749	0.3916	0.000017
	1.8356	1.8752	0.3994	0.000003
	1.8550	1.8756	0.4104	0.000000
Log law	1.8176	1.8678	0.5371	23.732740
	1.8356	1.8695	0.6135	33.681247
	1.8550	1.8716	0.7578	68.934686
(b) Tolerance level: 10^{-6}, number of iterations: 1,448, terminal time: 1.8732				
Power law	1.8172	1.8753	0.3927	0.000033
	1.8360	1.8757	0.4009	0.000006
	1.8547	1.8760	0.4118	0.000000
Log law	1.8172	1.8688	0.5500	25.226547
	1.8360	1.8705	0.6343	33.937325
	1.8547	1.8724	0.7854	58.894321

The initial condition (14) is taken with $a = 0.5$ and $b = 0$ when the initial velocity is $V(0) = -1.25$

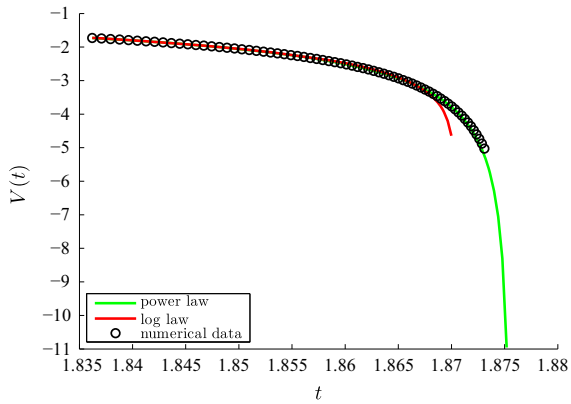

Fig. 7 Comparison between data fitting with the logarithmic law (8) and the power law (9)

In order to confirm that the blow-up of the velocity V occurs according to the power law (9) compared to the logarithmic law (8), we use the scaling transformations suggested in [4] and replace the time variable t by the new variable

$$T := \int_0^t (1 + V^{2k}(t'))\mathrm{d}t', \tag{25}$$

where k is a positive integer. In the new time variable with $V(t) \equiv V(T)$, the model (11) is rewritten in the form

$$\frac{\partial u}{\partial T} = \frac{1}{1 + V^{2k}} \left(V \frac{\partial u}{\partial x} - \frac{\partial^4 u}{\partial x^4} \right), \quad x > 0, \quad T > 0, \tag{26}$$

whereas the boundary conditions or the numerical method is unaffected. With the power law (9) as $t \nearrow t_0$, the new time variable T in (25) approaches a finite limit if $2kp < 1$ and becomes infinite if $2kp \geq 1$. With the logarithmic law (8), the new time variable T would always approach a finite limit for any integer k.

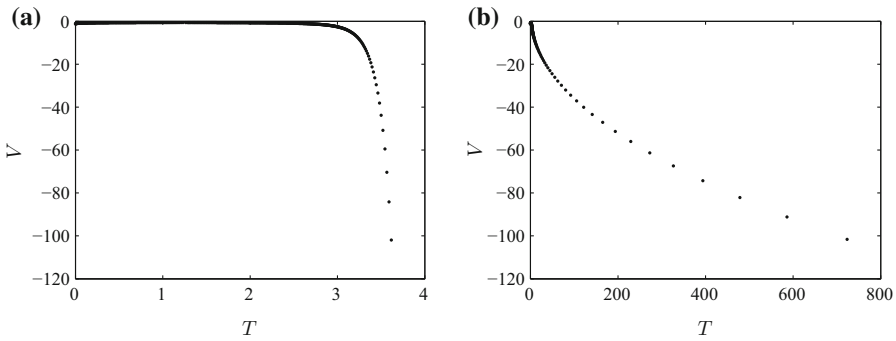

Fig. 8 Behavior of the velocity V versus T given by the scaling transformation (25) with **a** $k = 1$ and **b** $k = 2$

Table 2 Starting time, terminal time, regression slope q, and the blow-up rate p for numerical computations with rescaled time variable T

Starting time	Terminal time	Regression slope q	Blow-up rate p
36.0943	723.3424	0.5345	0.4697
121.7362	723.3424	0.5221	0.4797
272.5828	78034.1670	0.5044	0.4956
2393.6301	78034.1670	0.4997	0.5003

Figure 8 shows the dependence of V versus the rescaled time variable T for (a) $k = 1$ and (b) $k = 2$. It is obvious that the blow-up occurs in finite T time if $k = 1$ and in infinite T time if $k = 2$, which corroborates well with the previous numerical data suggesting that $0.25 < p < 0.5$. This figure rules out the validity of the logarithmic law (8). We have checked that the rescaled time variable T for $k \geq 3$ also extends to infinite times, similar to the result for $k = 2$.

We note that the dependence of V versus the original time variable t can be obtained by numerical integration of the integral in (25). We have checked that both time evolutions of V in T with $k = 1$ and $k = 2$ recover the same behavior of V in t, except near the blow-up time, where the computational error becomes more significant.

Using the scaling transformation (25) with $k = 2$ in the case when $T \to \infty$ as $t \to \infty$, we can define a more accurate procedure of detecting the blow-up rate p in the power law (9). First, we note that if $k = 2$ and $|V(t)| = \mathcal{O}((t_0 - t)^{-p})$ as $t \nearrow t_0$, then $T = \mathcal{O}((t_0 - t)^{1-4p})$ as $t \nearrow t_0$. Hence $V(T) = \mathcal{O}(T^q)$ as $T \to \infty$ with $q := p/(4p - 1)$. Using the linear regression in log–log variables for T and V, we can estimate the coefficient q, and then p.

Table 2 shows several computations of q and p for different initial and terminal times. All other parameters are fixed similarly to the previous numerical computations.

The results of data fitting in Table 2 suggest that the power law (9) gives a consistent estimation of the blow-up rate p, with $p \approx 0.5$. Let us now explain why the behavior $|V(t)| = \mathcal{O}((t_0 - t)^{-1/2})$ as $t \nearrow t_0$ is highly anticipated from the analysis of smooth solutions of the boundary-value problem (11)–(12).

Using Eqs. (13) and (19), we obtain the dynamical equation on $\beta(t) = u_x|_{x=0}$:

$$\frac{\mathrm{d}\beta}{\mathrm{d}t} = -\frac{u_{xxxx}\big|_{x=0}}{2\beta(t)} - u_{xxxxx}\big|_{x=0}, \quad t \geq 0. \tag{27}$$

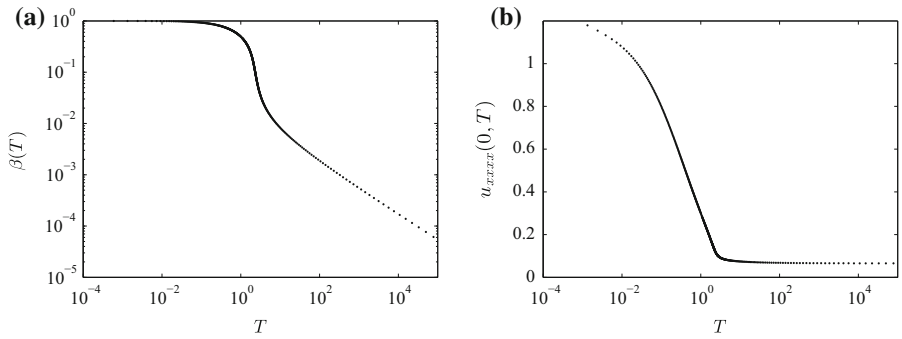

Fig. 9 Behavior of $|\beta|$ and $u_{xxxx}|_{x=0}$ versus T given by the scaling transformation (25) with $k = 2$. The logarithmic scaling is used for T and β variables. **a** $|\beta|$ versus T, **b** $u_{xxxx}|_{x=0}$ versus T

Let us now assume that there is $t_0 > 0$ such that

$$\beta(t) \to 0, \quad u_{xxxx}\big|_{x=0} \to a_4, \quad u_{xxxxx}\big|_{x=0} \to a_5 \quad \text{as} \quad t \nearrow t_0, \tag{28}$$

where $a_4 \neq 0$ and $|a_5| < \infty$. Solving the differential equation (27) near the time $t = t_0$, we obtain

$$\beta^2(t) = a_4(t_0 - t) + \mathcal{O}(t_0 - t)^{3/2} \quad \Rightarrow \quad |V(t)| = \sqrt{\frac{a_4}{t_0 - t}} + \mathcal{O}(1) \quad \text{as} \quad t \nearrow t_0, \tag{29}$$

under the constraint that $a_4 > 0$. The asymptotic rate (29) corresponds to the power law (9) with $p = 0.5$.

Figure 9 shows the behavior of absolute values of (a) $u_x|_{x=0}$ and (b) $u_{xxxx}|_{x=0}$ versus the rescaled time variable T given by (25) with $k = 2$. We can see that the assumption $a_4 > 0$, that is, $u_{xxxx}|_{x=0}$ is bounded away from zero near the blow-up time, is justified numerically. We note that the time evolution of $u_{xxxx}|_{x=0}$ in the rescaled time variable T allows us to identify this property better than the time evolution of this quantity in the original time variable t, which is shown in Figure 3(d). We have also checked from the linear regression in log–log coordinates that $|\beta(T)| = \mathcal{O}(T^{-q})$ as $T \to \infty$ with $q \approx 0.5$, that is, $|\beta(t)| = \mathcal{O}((t_0 - t)^p)$ as $t \nearrow t_0$ with $p \approx 0.5$, in consistence with the asymptotic rate (29).

5 Conclusion

We conclude from the numerical simulations of the boundary-value problem (11)–(12) that, for any suitable initial condition in the two-parameter form (14), there always exists a finite positive time t_0 such that $V(t) \to -\infty$ as $t \nearrow t_0$, although the blow-up time t_0 depends on the initial velocity $V(0)$. With a large positive initial velocity $V(0)$, the solution tends to have a longer phase of slow motion before it eventually blows up, whereas a negative initial velocity yields a much smaller value of the blow-up time.

The numerical results also suggest that the behavior of $V(t)$ near the blow-up time satisfies the power law (9), with a blow-up rate $p \approx 0.5$. This numerical observation corroborates a simple analytical theory for the blow-up of the velocity of contact lines in the reduced model (3)–(4). Based on earlier numerical evidences in [4], a similar result should also hold for the nonlinear thin-film equation (1).

Further studies of this phenomenon can be performed toward the development of a more computationally efficient numerical method for the boundary-value problem (11)–(12). Because the model equation (11) is already a fourth-order differential equation, we shall avoid using numerical methods that involve higher-order central differences. In addition, because of the unknown variable $V(t)$, it is difficult to use other higher-order implicit methods to solve the system of differential equations after discretization. Although the finite-difference method has thus a limited

efficiency, our results are not affected by this limitation because the adaptive method allows us to adjust the time step at each iteration and to control the same tolerance level throughout the simulations.

One possible new approach to numerical solution of this problem can be based on the spectral collocation method which can be implemented with either the Fourier expansion or the Chebyshev discretization. The difficulty in applying the Fourier expansion is the presence of the inhomogeneous boundary conditions in the boundary-value problem (11)–(12). If the domain is expanded in a periodic manner, the resulting Gibbs phenomenon at the boundaries will void the spectral accuracy of the Fourier method. On the other hand, the Chebyshev discretization seems to be more appropriate in this case, while the main difficulty still consists in incorporating the boundary conditions and solving a nonlinear equation for the evolution of $V(t)$. Implementations of the Chebyshev discretization method can be considered in the forthcoming studies.

Acknowledgments The work of D.P. was supported by the Ministry of Education and Science of Russian Federation (the base part of the state task No. 2014/133). The work of C. Xu was performed during an undergraduate project at the Department of Mathematics, McMaster University.

References

1. Benney DJ, Timson WJ (1980) The rolling motion of a viscous fluid on and off a rigid surface. Stud Appl Math 63:93–98
2. Pismen LM, Nir A (1982) Motion of a contact line. Phys Fluids 25:3–7
3. Ngan CG, Dussan VEB (1984) The moving contact line with a 180° advancing contact angle. Phys Fluids 24:2785–2787
4. Benilov ES, Vynnycky M (2013) Contact lines with a 180° contact angle. J Fluid Mech 718:481–506
5. Chugunova M, Pugh M, Taranets R (2010) Nonnegative solutions for a long-wave unstable thin film equation with convection. SIAM J Math Anal 42:1826–1853
6. Chugunova M, Taranets R (2012) Qualitative analysis of coating flows on a rotating horizontal cylinder. Int J Diff Equ 2012:570283
7. Pelinovsky DE, Giniyatullin AR, Panfilova YA (2012) On solutions of a reduced model for the dynamical evolution of contact lines. Trans Nizhni Novgorod State Tech Univ N.4(94):45–60
8. Pelinovsky DE, Giniyatullin AR (2012) Finite-time singularities in the dynamical evolution of contact lines. Bul Mosc State Reg Univ (Phys Math) 2012(3):14–24
9. Chugunova M, Kao CY, Seepen, S (2015) On Benilov–Vynnycky blow-up problem. Discr Cont Dyn Syst B (in press)